

# MEASUREMENT OF THE TRANSVERSE COHERENCE OF THE SASE FEL RADIATION IN THE OPTICAL RANGE USING AN HETERODYNE SPECKLE METHOD

M.D. Alaimo, M. Manfredda, V. Petrillo, M.A.C Potenza, D. Redoglio, L.Serafini  
Universita' and INFN-Mi, Milano, Italy

M. Artioli, F. Ciocci, A. Petralia, M. Quattromini, V. Surrenti, A. Torre, C. Ronsivalle  
ENEA C.R. Frascati, Frascati, Roma, Italy

L. Giannessi

ENEA C.R. Frascati, Frascati, Roma and Sincrotrone Trieste S.C.p.A., Trieste, Italy

J.V. Rau

ISM-CNR, Roma, Italy

M. Bellaveglia, E. Chiadroni, A. Cianchi, G. Di Pirro, G. Gatti, M. Ferrario, A. Mostacci,  
INFN-LNF, Frascati, Roma, Italy

## Abstract

We measured the transverse coherence of the SASE radiation an heterodyne speckle method at the SPARC FEL facility. The measure was done at the resonant wavelength  $\lambda_R = 400$  nm.

## INTRODUCTION

Novel research methods in the investigation of matter permit to reach the spatial resolution at atomic scales. The wave front uniformity and a high degree of transverse coherence (TC) of the radiation are fundamental in the applications where coherence based methods [1], such as intensity fluctuation spectroscopy, phase contrast imaging or holography, are involved. Free-Electron Lasers (FELs) [2, 3, 4] are among the most performing devices for producing radiation with short wavelength, high power, ultra-short time duration and large transverse and temporal coherence.

The transverse quality of the FEL beam, which is high also in the SASE regime and increases during the amplification process, besides being essential for user applications requiring tight focusing of light and intense illumination of the target, can also be used to access information about the FEL dynamics.

The degree of transverse coherence of the SASE FEL radiation, calculated using the statistical theory [7, 8], can be related to the emergence during the growth of specific TEM modes [9].

From an experimental and quantitative point of view, the TC of the FEL radiation has been first estimated by means of the Young's double slit fringes analysis through the Van Citter-Zernicke theorem [10, 13]. Wavefront analysis using the Hartmann technique was then proposed to determine the spatial characteristics of the FEL source in single-shot regime [11] and then demonstrated at the SCSS Test Accelerator using a specifically designed Hartmann Wavefront Sensor [14], and, more recently, on the FEL Fermi at Elettra [12]. Single-shot wavefront measurements were

performed directly on the FEL permitting to retrieve information about the FEL dynamics during the amplification, the beam optical quality, the source characteristics and the related instabilities from shot-to-shot.

Other methods of measuring the transverse coherence rely on the speckles generated by a sample of Brownian particles. After Fourier transform and proper normalization, the visibility of the fringes provides the same information as the traditional Young's double slit experiment for a continuous variation of pinhole distances. On the LCLS FEL an evaluation of the transverse coherence in the X ray range has been performed by measuring the homodyne speckle intensity due to coherent diffraction by disordered samples in the low and wide angle configurations (SAXS and WAXS respectively)[15]. By making assumptions about the shape of the beam profile, the first order statistical properties of the speckle patterns are related to the transverse and longitudinal coherence of the incoming radiation field, thus allowing to determine the field correlations and demonstrating the transverse coherence with a number of modes close to 1.

An alternative and powerful technique for the characterization of the two-dimensional transverse coherence has been developed and tested at the ESRF high brilliance undulator beamline ID02 and ID06 based on the measurement of the heterodyne speckle field generated by the scattering from a colloidal suspension of silica particles [16, 6].

In this paper we present the direct measures of the transverse coherence factor of the SASE FEL radiation with the aforementioned method in the optical range.

## EXPERIMENTAL SETUP

The experiment was performed at the SPARC FEL facility [4] with an electron beam whose main parameters are summarized in Table1 at the resonant wavelength  $\lambda_R = \frac{\lambda_u}{2\gamma^2}(1 + K^2/2) = 400$ , nm ( $\lambda_u$  being the undulator magnetic field period,  $K = eB_u\lambda_u/(2\pi m_e c)$  its deflection pa-

parameter and  $\gamma$  the Lorentz factor of the electrons).

Table 1: Main Electron Beam Parameters

Parameter	Value
Beam energy $E_B$ (MeV)	$162.5 \pm 0.27$
Beam charge (pC)	$312 \pm 16$
Energy Spread (proj.%)	$0.2 \pm 0.015$
Energy Spread (slice%)	$0.050 \pm 0.005$
Length r.m.s. (ps)	$1.65 \pm 0.05$
Beam current $I_{peak}$ (A)	$75.63 \pm 3.5$
Vertical Emittance 90% (mm mrad)	$1.95 \pm 1.0$
Horizontal Emittance 90% (mm mrad)	$1.74 \pm 1.1$

The electron bunch produced by the photoinjector with a current of about 75 A, was driven at 162.5 MeV by the linac and injected in the undulator system, consisting of six sections of 75 periods each, with  $\lambda_u = 2.8$  cm [17] at the resonant wavelength  $\lambda_R = 400$  nm. The SASE radiation was extracted after each undulator section and registered in intensity and spectrum by the SPARC spectrometer (an in-vacuum device [18] with normal incidence grating imaging the variable entrance slit on a UV grade CCD camera, Versarray, 1300B-Princeton Instruments). A typical spectrum at the end of the undulator is presented in Fig. 1.

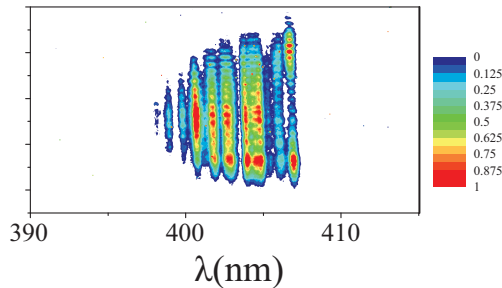


Figure 1: Spectro-spatial image of the radiation at the end of the undulator. The vertical axis on the image of the spectra represents the vertical position on the input spectrometer slit.

The experimental energy growths of the radiation along the undulator and the simulation performed with the code GENESIS 1.3 [19] are reported in Fig. 2. The radiation shows the characteristic behavior of the exponential growth, with a measured gain length of about  $L_g = \frac{\lambda_u}{4\pi\rho} = 1.31$  m,  $\rho$  being the Pierce parameter.

The diagnostic set-up for transverse coherence measurements is very similar to the in-line holography scheme. The FEL radiation illuminates a sample of colloidal particles in water suspension and the interference between the transmitted and the scattered field is recorded by a CCD camera placed at a distance  $z=13$  cm from the sample (Fig. 3). The sample is composed by a 2 mm thick optical cell containing commercial polystyrene particles ( $n=1.63$ ) with a diameter  $d=2.1 \mu\text{m}$  at low concentration. The CCD camera is a 14bit PCO1600 with a resolution of  $1600 \times 1200$  and a pixel size

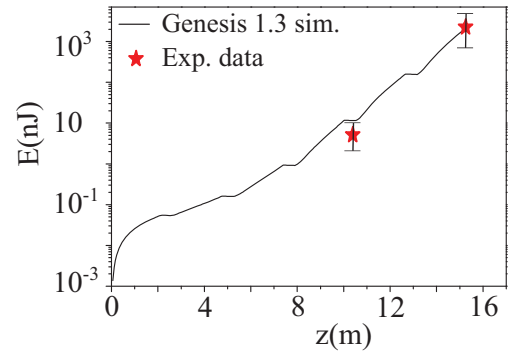


Figure 2: Radiation characteristics at the end of the undulator, experimental (red stars) and simulated (solid lines) (simulations by GENESIS 1.3 [19] made with parameters as Table 1).

of  $d_{px} = 7,4 \mu\text{m}$ .

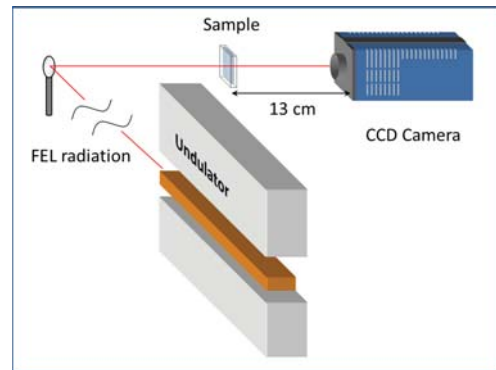


Figure 3: Speckle diagnostics set-up.

## DATA ANALYSIS

The complex coherence factor (CCF) is usually introduced through the second-order transverse correlation function:

$$\gamma(\underline{r}_{\perp,1}, \underline{r}_{\perp,2}) = \frac{\langle \tilde{E}^*(\underline{r}_{\perp,1}, t) \tilde{E}(\underline{r}_{\perp,2}, t) \rangle}{\sqrt{\langle |\tilde{E}(\underline{r}_{\perp,1}, t)|^2 \rangle \langle |\tilde{E}(\underline{r}_{\perp,2}, t)|^2 \rangle}} \quad (1)$$

where  $\tilde{E}$  is the amplitude of the amplified wave, according to the SVEA approximation and the symbol  $\langle \rangle$  denotes the average on time. Assuming that the random process is stationary,  $\tilde{E}$  is not time-depending and  $\gamma$  coincides with the transverse equal time correlation function. Following [9], the transverse coherence degree turns out to be

$$\varsigma = \frac{\int |\gamma(\underline{r}_{\perp,1}, \underline{r}_{\perp,2})|^2 I(\underline{r}_{\perp,1}) I(\underline{r}_{\perp,2}) d\underline{r}_{\perp,1} d\underline{r}_{\perp,2}}{[\int I(\underline{r}_{\perp,1}) d\underline{r}_{\perp,1}]^2} \quad (2)$$

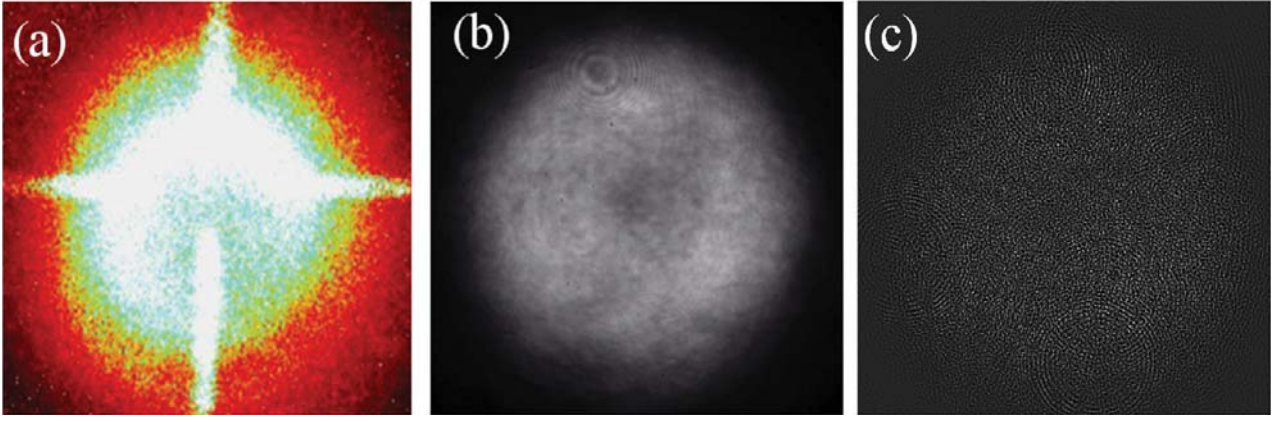


Figure 4: (a) Electron beam and radiation taken on a phosphorous screen after the fifth section of the undulator (b) Transmitted pulse plus scattered field, and (c) heterodyne speckle function  $s(\underline{r})$  after background subtraction at the end of the undulator.

where  $I = |\tilde{E}|^2$  is the radiation intensity. Simulations made by GENESIS 1.3 gives a value of  $\zeta$  for our the source almost equal to 1 (fully coherent beam).

Experimentally the Fourier analysis of the field scattered by the colloidal sample brings to  $|\gamma(R)|$ , where  $R = r_{\perp,1} - r_{\perp,2}$  and the evaluation of the parameter  $\zeta$  can be done by the direct comparison between the width of the CCF and the beam size.

An electron beam trace taken on a phosphorous screen after the sixth undulator is presented in Fig 4.a. The radiation exiting from the SPARC undulator impinges on the sample and it is recorded by the CCD camera. The row signal is presented in Fig.4.b.

The intensity  $I$  recorded by the camera is given by the interference of the transmitted wave and the field diffracted by the suspension. It can be written as:

$$I(\underline{r}) \approx I_{FEL}(\underline{r}) + 2\text{Re}[E_{FEL} * (\underline{r}) E_s(\underline{r})] \quad (3)$$

where  $E_{FEL}(\underline{r})$  is the FEL transmitted field,  $I_{FEL}$  the corresponding intensity and  $E_s(\underline{r})$  the wave scattered by the sample (the asterisk indicates complex conjugation). Since the particle concentration is very low ( $E_s \ll E_{FEL}$ ) a quadratic term  $|E_s(\underline{r}) E_s^*(\underline{r})|$  has been neglected. The second term of Eq.3 represent the so called "heterodyne signal" and brings information about the coherence properties of the radiation. In order to isolate this term a background subtraction can be done by evaluating the difference between two images  $I_1(\underline{r})$  and  $I_2(\underline{r})$  taken at different times  $t_1 - t_2 = \Delta t$ . The quantity  $s(\underline{r}) = (I_1 - I_2)$  translates in:  $s(\underline{r}) \approx \text{Re}[E_{FEL} * (E_{s1} - E_{s2})]$ . Fig.4.c shows the quantity  $s(\underline{r})$ . The typical granular pattern (speckle field) which is the result of the stochastic interference of the fields scattered by the particles can be seen.

Once  $s(\underline{r})$  is obtained, the two-dimensional power spectrum  $S(q) = |\int s(\underline{r}) \exp(-iq \cdot \underline{r}) d\underline{r}|^2$  can be numerically evaluated, where  $\underline{q}$  is the scattering wave vector defined for a small scattering angle,  $\theta$ , as  $q = k\theta$  ( $k = 2\pi/\lambda$ )(Fig.5). It can be shown that:

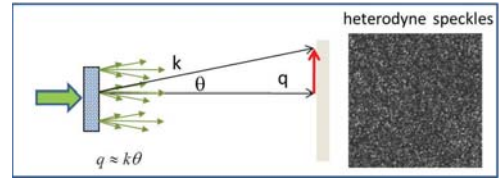


Figure 5: Detail of the speckle field obtained at the exit of the sample on the CCD camera and scattering geometry.

$$S(q) = C(q)T(q)I(q) \quad (4)$$

where  $I(q)$  is the two-dimensional scattered intensity distribution (almost flat in the  $q$ -range accessible for the setup) and  $T(q) = \sin^2(q^2 z / 2k)$  is the Talbot transfer function that can be evaluated theoretically [16, 6]. The complex coherence factor is given by  $C(R) = |\gamma(R)|^2$  after operating the rescaling  $R = zq/k$ . An example of the speckle field and the geometry of the system are presented in Fig. 5. One tricky step of the data analysis scheme is represented by the choose of the time interval  $\Delta t$  between the two images used for the evaluation of the quantity  $s(\underline{r})$ . In fact the power spectrum of  $s(\underline{r})$  is given by Eq.4 only under the hypothesis that the field  $E_{s1}$  and  $E_{s2}$  are completely uncorrelated. The changing in the scattering field is related to the changing of the particles position in the sample due to diffusion, convection or sedimentation. It turns out that in our case the most important effect is given by convection and a time delay of the order of 200-300 seconds is enough for the complete decorrelation. The bidimensional  $S(q)$  has been evaluated for the SPARC FEL radiation. Since the the CCF reveals a rotational symmetry, we show in Fig.6 its azimuthal average (red-blue line). Oscillations introduced by the Talbot transfer function are visible for low  $R$  values (which corresponds to low  $q$  vectors) and disappear approximately at  $R=2$  mm. Besides this value, the spatial frequency of the oscillations becomes

higher than the Nyquist frequency for our system and the transfer function becomes flat. It is possible to point out an unphysical behavior of the function (blue line) for very low R values ( $R < 1$  mm) where  $S(q)$  is much higher than 1. This behavior is not connected to the coherence properties of the radiation but, rather, to beam instabilities. Due to typical SASE instabilities or mechanical vibration, the beam position changes slightly from shot to shot, leading to the presence of a spurious term in  $S(R)$  essentially related to the typical fluctuation in the beam position. The analysis of the beam positions, operated on the same set of images used for the coherence measurement, suggests that the effect of the beam instabilities can be neglected for  $R > 1$  mm. In this range of values the CCF is impressively well fitted with a Gaussian function (black line). Estimate of  $\zeta$  leads to a value slightly higher than 0.8.

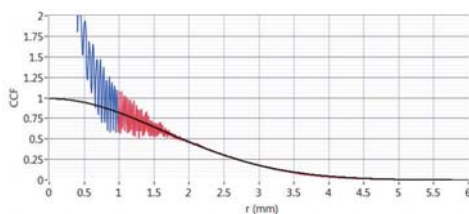


Figure 6: Fourier analysis of the heterodyne speckles field (red-blue curve) and Gaussian fit (black curve).

With a different analysis on the same set of images the total number of modes in a single FEL pulse can be evaluated. Defining  $W$  the total energy in a single pulse, for the first order statistic holds:

$$\rho(W) = \frac{M^M}{\Gamma(M) \langle W \rangle} \left( \frac{W}{\langle W \rangle} \right)^{M-1} e^{-M \frac{W}{\langle W \rangle}} \quad (5)$$

where  $\Gamma(M)$  is the gamma function with argument  $M = 1/\sigma_W^2$ , and  $\sigma_W^2 = (W - \langle W \rangle)^2 / W^2$  is the relative dispersion of the radiation energy [9].

The statistical analysis made over 1200 events is shown in Fig. 7 together with the gamma function evaluated using the signal mean and variance with no free parameters. The estimated number of longitudinal coherence areas, as given by  $M$ , is 3.3, in good agreement with the fringe number shown by the experimental spectral measurements.

## CONCLUSION

The direct measure of the transverse coherence factor of the SASE FEL radiation based on the detection and analysis of the speckle field generated from the scattering from a colloidal suspension of silica particles in the SPARC FEL has been presented. At the end of the undulator, corresponding in our case to the final stage of the exponential growth, an almost total transverse coherence has been found, with a TC degree larger than 0.8.

ISBN 978-3-95450-123-6

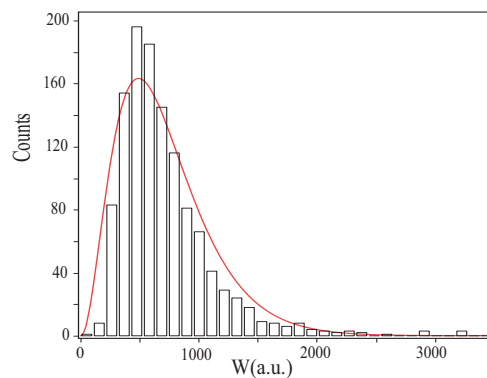


Figure 7: Fourier analysis of the heterodyne speckles field (red-blue curve) and Gaussian fit (black curve).

## ACKNOWLEDGMENT

The authors gratefully acknowledge Prof. M. Giglio and G. Geloni for their interest and support and the whole SPARC Team for long hours spent in the control room for making this experiment possible.

## REFERENCES

- [1] D. Mills et al., "Third Generation Hard X-Ray Synchrotron Radiation Sources", John Wiley and Sons, Inc., New York (2002).
- [2] Z. Huang et al., Phys. Rev. ST Acc. Beams, 13, (2010) 020703.
- [3] W. Ackermann et al., Nat. Photonics, 1, (2007) 336.
- [4] L. Giannessi et al., Phys. Rev. ST Acc. Beams 14, (2011) 060712.
- [5] T. Shintake et al., Nat. Photon. 2, (2008) 555.
- [6] M. Manfreda et al., in preparation.
- [7] K.-J. Kim, Phys. Rev. Lett. 57, (1986) 1871.
- [8] G. Geloni et al., New J. Phys 12, (2010) 035021.
- [9] E. L. Saldin et al., Opt. Commun. 148, (1998) 383.
- [10] R. Ischenbeck et al., Nucl. Instr. Meth. Phys. Res. A 507, (2003). 175.
- [11] P. Mercere et al., in 2009 FEL International Conference (Liverpool), pg 72 (2009).
- [12] L. Giannessi, private communication.
- [13] A. Singer, Phys. Rev. Lett. 101, (2008) 254801.
- [14] R. Bachelard et al., Phys. Rev. Lett. 106, (2011) 234801.
- [15] C. Gutt et al., Phys. Rev. Lett. (2012) 024801.
- [16] M.D. Alaimo et al. Phys. Rev. Lett. 103, (2009) 194805.
- [17] M. Quattromini et al., in Proceedings of the 2008 EPAC Conference (www.jacow.org, 2008), p. WEPC124.
- [18] L. Poletto et al., Rev. Sci. Instr. 75, (2004) 4413.
- [19] S. Reiche, Nucl. Instrum. and Meth. in Phys. Res. A 429, (1999). 243